

$U(1)$ -Symmetry protected Dirac nodal loops of triplons in $\text{SrCu}_2(\text{BO}_3)_2$

Dhiman Bhowmick[✉] and Pinaki Sengupta[✉]
*School of Physical and Mathematical Sciences,
Nanyang Technological University,
21 Nanyang Link, Singapore 637371, Singapore*

(Dated: March 31, 2020)

We demonstrate the appearance of symmetry protected triplon Dirac modal lines in the low energy excitation spectrum of a realistic microscopic model of the geometrically frustrated quantum magnet $\text{SrCu}_2(\text{BO}_3)_2$ in its high symmetry phase. The symmetry-allowed Dzyaloshinskii-Moriya interactions induce dispersive triplon bands within the bond-operator formalism that cross linearly over an extended closed path in the Brillouin zone. Our results establish that the nodal lines are protected by a $U(1)$ -symmetry and robust against perturbations that preserve this symmetry. In the presence of a longitudinal field, the nodal loop shrinks and vanishes for a sufficiently strong field.

I. INTRODUCTION

The study of topological phases of matter has grown into one of the most active frontiers of contemporary condensed matter physics. Recently, the experimental observation of Weyl fermions in TaAs[1], building upon previous theoretical studies[2, 3], has generated widespread interest in topological semimetals. In these systems, a linear crossing of two bands at one or more points in momentum space is topologically protected. Following the discovery of TaAs, materials with Dirac nodal lines or nodal loops were discovered where the linear band crossing exists over an extended region in the Brillouin zone (BZ), thus expanding the types of semimetals[4–15]. The nodal lines or loops in these systems is protected by the presence of certain symmetries like inversion[7, 16, 17], mirror-reflection[6, 12, 13, 18] or glide-plane[19–21]. Since topological phases are often manifestations of the geometry of the band structure which do not depend on the quantum statistics of the quasi-particles involved, efforts to realize bosonic analogs of topological phases have gained interest in the recent past. Bosonic counterparts of the topological phenomena have been explored in wide ranging bosonic systems such as photons[22, 23], exciton-polaritons[24, 25], magnons[26–43], magnon-polarons[44–47]. Quantum magnets, in particular, offer a promising route to search for novel topological phases of quantized magnetic excitations such as magnons and triplons that obey Bose-Einstein statistics.

The band structure geometry that drives topological properties is largely determined by the symmetries of the lattice and the Hamiltonian. While fermionic phases are governed by lattice space group symmetries, magnetic systems are governed by a richer magnetic symmetry group, whose elements consist of products of a space group symmetry operation and the time reversal operation. The geometry of the band structure of magnetic quasiparticle excitations are governed by elements of the magnetic symmetry group. Dirac magnon nodal lines that are protected by simultaneous inversion (\mathcal{P}) and time reversal (\mathcal{T}) symmetry have been predicted

to appear in anisotropic pyrochlore ferromagnets[48], the spin-web compound Cu_3TeO_6 [49] and layered honeycomb antiferromagnets[50].

Moreover, the nodal line semimetals are mostly studied theoretically and experimentally in the three dimensional systems. However, recently it has been shown the two dimensional counterpart for Dirac nodal lines also exist[51–54]. Although as a bosonic counterpart the presence of Dirac nodal line in the magnetic excitations of a quasi-2D ferromagnetic honeycomb lattice has been investigated[55], but as far as our knowledge no studies show the presence of Dirac nodal line magnetic excitation in completely two-dimensional magnetic system without interlayer coupling.

In this work, we investigate the high symmetry crystal phase of the geometrically frustrated quantum magnet $\text{SrCu}_2(\text{BO}_3)_2$ and demonstrate the appearance of field induced Dirac nodal loops in triplon bands for perfectly 2D-system. Previous studies for nodal line magnons have been restricted to excitations above ground states with classical (static) spin ordering [48–50]. In contrast to those studies, we have explored magnetic excitations in the dimerized phase of the Shastry-Sutherland model (with additional DM (DM) interactions). To the best of our knowledge, ours is the first study to show that Dirac nodal line also can exist in the excitation spectrum of purely quantum-mechanical ground state with only short range order. The high-symmetry phase of $\text{SrCu}_2(\text{BO}_3)_2$ consists of weakly coupled layers in which the Cu^{2+} ions are arranged in an orthogonal dimer configuration constituting the non-symmorphic Shastry-Sutherland lattice[56]. The space group of $\text{SrCu}_2(\text{BO}_3)_2$ is $I4/mcm$ in the high symmetry phase (at high temperatures) and is reduced to $I42m$ at $T = 395\text{K}$ via a structural transition[57, 58]. The symmetry determines the allowed terms in the Hamiltonian, in particular, the nature of Dzyaloshinskii-Moriya (DM) interactions[59].

The dominant (magnetic) interaction in $\text{SrCu}_2(\text{BO}_3)_2$ is antiferromagnetic Heisenberg superexchange between Cu^{2+} ions across intra- and inter-dimer bonds. In the high symmetry phase, DM interaction is allowed only on the inter-dimer bonds with the DM vector normal to the

plane, which preserves the $U(1)$ -symmetry of the spin-system[59]. The ground state of $\text{SrCu}_2(\text{BO}_3)_2$ is well approximated by the dimer singlet phase where the spins on each dimer form a singlet[59–62]. In the absence of DM interactions, the lowest excitation would consist of 3-fold degenerate dispersionless triplons on the dimer bonds. In the presence of DM interactions, the triplon bands acquire finite dispersion and non-zero Berry curvature. The nature of DM interactions determine the evolution of the triplon bands in an external magnetic field. This has been extensively investigated in the low-symmetry phase of $\text{SrCu}_2(\text{BO}_3)_2$ where upon the application of a longitudinal magnetic field a gap opens up in the spectrum and the bands acquire a non-zero Chern number[63–65]. In this work we investigate the triplon bands in the high symmetry phase of $\text{SrCu}_2(\text{BO}_3)_2$ in an external longitudinal magnetic field. Our results show that in this phase, the triplon bands exhibit Dirac nodal loop which is protected by $U(1)$ -symmetry. When a longitudinal field is turned on, the nodal loop shrinks continually with increasing field and eventually disappears at a critical field with the opening of a gap. We analyze the mechanism of emergence and properties of the Dirac nodal loop within the framework of bond operator formalism.

II. MODEL AND METHOD

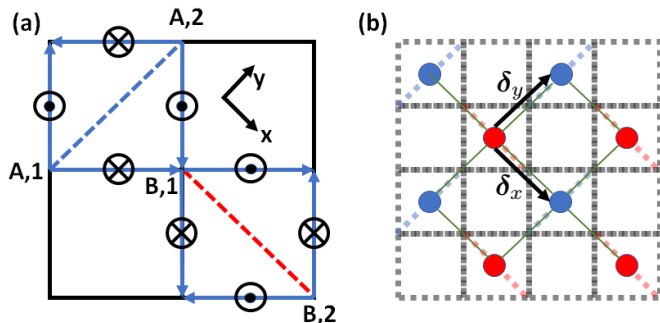


FIG. 1: **The Shastry-Sutherland lattice.** (a) The schematic of Shastry-Sutherland lattice. The circled-dots(circled-crosses) represent the perpendicular DM-interaction out of(into) the plane of paper. The dotted blue line and dotted red line represent the dimer-bond A and dimer-bond B of the lattice respectively. (b) The effective square lattice structure after bond-operator transformation. The dimer-bonds convert into points and on each point only one quasi-particle triplon can reside. The dimer-A is converted into blue dot and dimer-B is converted into red dot.

The figure Fig.1(a) illustrates the Shastry-Sutherland lattice including the DM-interactions present in the high symmetry phase of $\text{SrCu}_2(\text{BO}_3)_2$. The Hamiltonian of

the system is given by,

$$\mathcal{H} = J' \sum_{\langle i,j \rangle_d} \mathbf{S}_i \cdot \mathbf{S}_j + J \sum_{\langle i,j \rangle_{x,y}} \mathbf{S}_i \cdot \mathbf{S}_j + \mathbf{D}_\perp \cdot \sum_{\langle i,j \rangle_{x,y}} (\mathbf{S}_i \times \mathbf{S}_j) - g_z h_z \sum_i \mathbf{S}_i^z, \quad (1)$$

where $\langle \dots \rangle_{x,y}$, $\langle \dots \rangle_d$ denote the summation over the sites belonging to intra- and inter-dimer bonds respectively. J and J' denote the strengths of the corresponding Heisenberg interaction terms. \mathbf{D}_\perp is the DM-interaction shown as in Fig.1(a). The fourth term is the Zeeman coupling of the spins with the magnetic field h_z perpendicular to the Shastry-Sutherland layer with Lande-g factor g_z . The theoretical studies in Ref.[63–65] shows a vast phase diagram as well as the topological properties of the magnetic excitations. We show that the presence of $U(1)$ -symmetry and the DM-interaction D_\perp in the material give rise to $U(1)$ -symmetry protected Dirac-nodal line in the bands of low lying magnetic excitations in the system.

In the absence of DM-interactions, the possible ground states of the Shastry-Sutherland lattice are dimer phase, Néel phase and plaquette-singlet phase. The dimer phase of the Shastry-Sutherland lattice exists for $J' \lesssim 0.7J$ [60–62]. The singlet dimer phase of Shastry-Sutherland lattice is experimentally realized in $\text{SrCu}(\text{BO}_3)_2$, where the Cu^{2+} carries spin-1/2 degrees of freedom and forming a orthogonal dimer model[57, 66–68]. The chosen DM-interactions are symmetry allowed for the high symmetry phase of $\text{SrCu}_2(\text{BO}_3)_2$ [57, 58, 63]. In the presence of DM-interaction the dimer-singlet phase persists as the ground state for a finite parameter range $-0.2 \lesssim D_\perp/J \lesssim 0.2$ [59]. In this study we show that the presence of $U(1)$ -symmetry and perpendicular DM-interaction D_\perp gives rise to Dirac nodal line of the low lying magnetic excitations of this system.

The ground state of the canonical Shastry-Sutherland model in the large J/J' regime (applicable to $\text{SrCu}_2(\text{BO}_3)_2$) is a product of singlet-dimer states on the red and blue-bonds(Fig.1(b)). Hence it is natural to use the bond operator formalism to study the Hamiltonian (1). The local Hilbert space on a single dimer consists of a singlet $|s\rangle = (|\uparrow\downarrow\rangle - |\downarrow\uparrow\rangle)/\sqrt{2}$ and three triplons $|t_x\rangle = i(|\uparrow\uparrow\rangle - |\downarrow\downarrow\rangle)/\sqrt{2}$, $|t_y\rangle = (|\uparrow\uparrow\rangle + |\downarrow\downarrow\rangle)/\sqrt{2}$ and $|t_z\rangle = -i(|\uparrow\downarrow\rangle + |\downarrow\uparrow\rangle)/\sqrt{2}$. In this basis, the bare spin operators are represented as[69],

$$\hat{S}_{j,1}^\alpha = \frac{i}{2} \left(\hat{t}_j^{\alpha\dagger} \hat{s}_j - \hat{s}_j^\dagger \hat{t}_j^\alpha \right) - \frac{i}{2} \epsilon_{\alpha,\beta,\gamma} \hat{t}_j^{\beta\dagger} \hat{t}_j^\gamma, \\ \hat{S}_{j,2}^\alpha = -\frac{i}{2} \left(\hat{t}_j^{\alpha\dagger} \hat{s}_j - \hat{s}_j^\dagger \hat{t}_j^\alpha \right) - \frac{i}{2} \epsilon_{\alpha,\beta,\gamma} \hat{t}_j^{\beta\dagger} \hat{t}_j^\gamma, \quad (2)$$

where α , β or γ represent x , y or z . The operator $\hat{S}_{j,k}^\alpha$ represents the spin operator at site- k (site-1 or site-2) of dimer- j (dimer-A or dimer-B), see Fig.1; $\hat{t}_j^{\alpha\dagger}$ and \hat{s}_j^\dagger are the triplon and singlet creation operators at j -th dimer.

The triplon and singlet operators are bosonic quasiparticles and obey the following constraint on each dimer-bonds,

$$\hat{s}_j^\dagger \hat{s}_j + \sum_j \hat{t}_j^{\alpha\dagger} \hat{t}_j^\alpha = 1 \quad (3)$$

The ground state of the Hamiltonian (1) is well approximated by a condensation of singlets on the dimer bonds. In the bond operator formalism, this is implemented as $\langle \hat{s}_j^\dagger \rangle = \langle \hat{s}_j \rangle = 1$. The lowest excitations are isolated triplons on each dimer. Assuming a low density of triplons, we can derive a minimal model for the triplons by applying the bond operator formalism together with the constraint (3), and the condition $\langle \hat{s}_j^\dagger \rangle = \langle \hat{s}_j \rangle = 1$ to the parent Hamiltonian (1),

$$\begin{aligned} \mathcal{H} = & J \sum_{\mathbf{r}_i} [\hat{t}_{\mathbf{r}_i}^{x\dagger} \hat{t}_{\mathbf{r}_i}^x + \hat{t}_{\mathbf{r}_i}^{y\dagger} \hat{t}_{\mathbf{r}_i}^y + \hat{t}_{\mathbf{r}_i}^{z\dagger} \hat{t}_{\mathbf{r}_i}^z] \\ & + ig_z h_z \sum_{\mathbf{r}_i} [\hat{t}_{\mathbf{r}_i}^{x\dagger} \hat{t}_{\mathbf{r}_i}^y - \hat{t}_{\mathbf{r}_i}^{y\dagger} \hat{t}_{\mathbf{r}_i}^x] \\ & - \frac{iD_\perp}{2} \sum_{\mathbf{r}_i} \sum_{\boldsymbol{\delta}} [\hat{t}_{\mathbf{r}_i+\boldsymbol{\delta}}^{x\dagger} \hat{t}_{\mathbf{r}_i}^x - \hat{t}_{\mathbf{r}_i+\boldsymbol{\delta}}^{x\dagger} \hat{t}_{\mathbf{r}_i}^y + \text{h.c.}], \quad (4) \end{aligned}$$

where we have used a mean field decomposition to keep terms up to bilinear in the triplon operators. Again \mathbf{r}_i is the position vector of the i -th dimer and $\boldsymbol{\delta}_x$ or $\boldsymbol{\delta}_y$ are the vectors denoting the relative positions of the dimers as depicted in Fig.1(b). The triplons hop on an effective square lattice as shown in the figure Fig.1(b). It is further noted that in the Hamiltonian (4), the sites corresponding to dimer-A and dimer-B are mapped to a equivalent site using the following unitary transformation $t_{\mathbf{r}_i,A}^x = t_{\mathbf{r}_i}^x$, $t_{\mathbf{r}_i,A}^y = t_{\mathbf{r}_i}^y$, $t_{\mathbf{r}_i,A}^z = t_{\mathbf{r}_i}^z$, $t_{\mathbf{r}_i,B}^x = it_{\mathbf{r}_i}^x$, $t_{\mathbf{r}_i,B}^y = it_{\mathbf{r}_i}^y$, $t_{\mathbf{r}_i,B}^z = t_{\mathbf{r}_i}^z$. Moreover for simplicity we have neglected the pair hopping terms which changes the energy perturbatively to the order of D_\perp^2 and hence do not change the band structure[63]. Since the Hamiltonian (4) is translationally invariant, it is natural to work in the momentum space. The momentum space triplon-Hamiltonian is given as,

$$\mathcal{H} = \sum_{\mathbf{k}} \begin{pmatrix} \hat{t}_{\mathbf{k}}^{x\dagger} \\ \hat{t}_{\mathbf{k}}^{y\dagger} \\ \hat{t}_{\mathbf{k}}^{z\dagger} \end{pmatrix} \begin{pmatrix} J & -i\gamma(\mathbf{k}) & 0 \\ i\gamma(\mathbf{k}) & J & 0 \\ 0 & 0 & J \end{pmatrix} \begin{pmatrix} \hat{t}_{\mathbf{k}}^x \\ \hat{t}_{\mathbf{k}}^y \\ \hat{t}_{\mathbf{k}}^z \end{pmatrix}, \quad (5)$$

where $\gamma(\mathbf{k}) = -g_z h_z + D_\perp (\cos(k_x) + \cos(k_y))$. The following canonical transformation of the triplon operators,

$\hat{t}_{\mathbf{k}}^{x\dagger} = \frac{i}{\sqrt{2}} (\hat{t}_{\mathbf{k}}^{1\dagger} - \hat{t}_{\mathbf{k}}^{\bar{1}\dagger})$, $\hat{t}_{\mathbf{k}}^{y\dagger} = \frac{1}{\sqrt{2}} (\hat{t}_{\mathbf{k}}^{1\dagger} + \hat{t}_{\mathbf{k}}^{\bar{1}\dagger})$, $\hat{t}_{\mathbf{k}}^{z\dagger} = -i\hat{t}_{\mathbf{k}}^{0\dagger}$ diagonalizes the Hamiltonian Eq5 as,

$$\mathcal{H} = \sum_{\mathbf{k}} \begin{pmatrix} \hat{t}_{\mathbf{k}}^{\bar{1}\dagger} \\ \hat{t}_{\mathbf{k}}^{0\dagger} \\ \hat{t}_{\mathbf{k}}^{1\dagger} \end{pmatrix} \begin{pmatrix} J - \gamma(\mathbf{k}) & 0 & 0 \\ 0 & J & 0 \\ 0 & 0 & J + \gamma(\mathbf{k}) \end{pmatrix} \begin{pmatrix} \hat{t}_{\mathbf{k}}^{\bar{1}} \\ \hat{t}_{\mathbf{k}}^0 \\ \hat{t}_{\mathbf{k}}^1 \end{pmatrix}, \quad (6)$$

where the operators $\hat{t}_{\mathbf{k}}^{\bar{1}\dagger}$, $\hat{t}_{\mathbf{k}}^{0\dagger}$ and $\hat{t}_{\mathbf{k}}^{1\dagger}$ create the states $|t^{\bar{1}}\rangle = |\uparrow\uparrow\rangle$, $|t^0\rangle = (|\uparrow\downarrow\rangle + |\downarrow\uparrow\rangle)$ and $|t^1\rangle = |\downarrow\downarrow\rangle$ on the dimer respectively. As a consequence of $U(1)$ -symmetry conservation \hat{S}_z is also a eigen-operator of the eigenstates $|t^{\bar{1}}\rangle$, $|t^0\rangle$ and $|t^1\rangle$ and the S_z -quantum numbers corresponding to the states are $-1, 0, +1$ respectively.

III. RESULTS

We have chosen the Hamiltonian parameters as estimated for $\text{SrCu}_2(\text{BO}_3)_2$, viz., $J = 722$ GHz, $D_\perp = -21$ GHz and $g_z = 2.28$ [63, 70]. Using these parameters, we have studied the evolution of the triplon bands in a longitudinal magnetic field, h_z . The band dispersion for different magnetic fields are depicted in Fig.2(a)-(e). The spectrum consists of one dispersionless, flat band and two dispersive bands. At zero magnetic field, the two dispersive bands cross linearly at all points along the perimeter of a quadrilateral formed by joining the four X points on the Brillouin Zone boundary, shown by the green lines in Fig.2(f). The dispersion of lower or upper bands near nodal line up to second order of k_\perp and k_\parallel is given by, $J \pm D_\perp |k_\perp|$, where k_\parallel and k_\perp denotes the momentum in the direction parallel and perpendicular to the Dirac nodal line respectively. The Dirac nodal line persists over a finite range of magnetic field $-h_c < h_z < h_c$, where $h_c = \frac{2D_\perp}{g_z}$. Away from $h_z = 0$ (and for $|h_z| < h_c$), the Dirac nodal line forms a closed loop for any nonzero h_z -value centered around Γ or M -point in the Brillouin zone. For $\text{sgn}(D_z h_z) > 0$ ($\text{sgn}(D_z h_z) < 0$) the closed loop centers around Γ (M) point. When the magnetic field h_z is close to $\pm h_c$ the Dirac nodal line forms a circle with radius $k = \cos^{-1} \left(-1 + \left| \frac{g_z h_z}{D_\perp} \right| \right)$. The dispersion near the nodal line for the upper or lower bands up to second order of k_\perp and k_\parallel are $J \pm D_\perp \sin(k) |k_\perp| \pm \frac{D_\perp}{2} k_\parallel^2$, where k_\perp and k_\parallel denote the k -points in direction perpendicular and parallel to the circumference of the nodal line. At the critical magnetic field $\pm h_c$, the Dirac nodal line shrinks to a quadratic band touching point and for magnetic field $|h_z| > |h_c|$ the triplon bands become gapped.

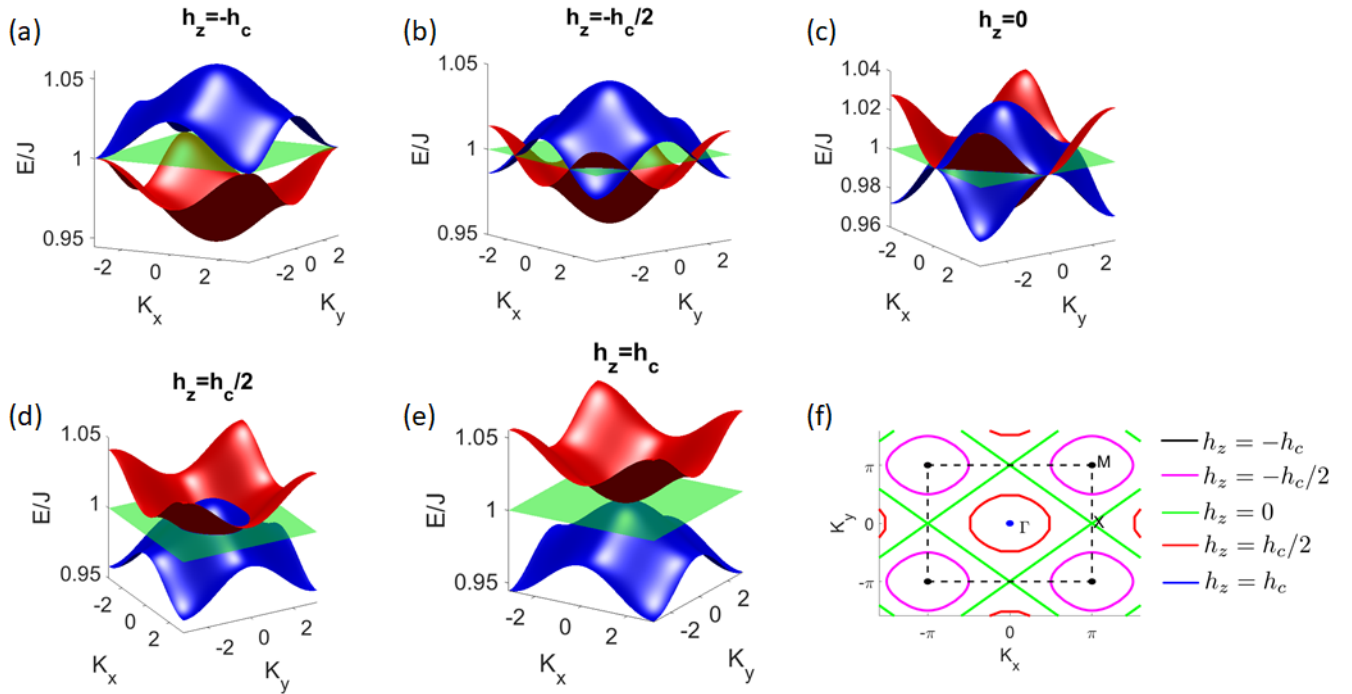


FIG. 2: **Dirac nodal line magnons.** (a)-(e) The triplon band structure for different magnetic fields. The colors blue, green and red denote the triplon eigenstates $|t^1\rangle$, $|t^0\rangle$ and $|t^1\rangle$ respectively. For better visibility, the middle band is kept transparent. (f) The k-space position of Dirac nodal line for different magnetic fields.

IV. SYMMETRY CONSIDERATIONS

The Dirac nodal line in the triplon band structure is robust against the perturbation from inversion symmetry breaking term (e.g. the different Heisenberg interaction for dimer-A and dimer-B) as well as time reversal symmetry breaking term (e.g. perpendicular magnetic field). But any perturbation which breaks the $U(1)$ -symmetry lifts the degeneracy at Dirac nodal line. Physically the bond-operator formalism translates the spin model of Shastry-Sutherland lattice into a simple effective square lattice model (Fig.1(b), Eq.4) with three orbitals $|t^1\rangle$, $|t^0\rangle$ and $|t^1\rangle$ on each lattice site. The presence of $U(1)$ -symmetry ensures that the inter-species hopping in the square lattice is disallowed. In other words, the nodal loop exists due to $U(1)$ -symmetry.

We define the following \mathbb{Z} -topological invariant for the $U(1)$ -symmetry protected Dirac nodal line [71, 72],

$$\Delta S_z = \langle \hat{S}^z(\mathbf{k}_{in}) \rangle - \langle \hat{S}^z(\mathbf{k}_{out}) \rangle, \quad (7)$$

where \mathbf{k}_{in} and \mathbf{k}_{out} are the k-points inside and outside of the Dirac nodal loop. Again $\langle \hat{S}^z(\mathbf{k}_l) \rangle$ is the eigenvalue of \hat{S}^z at \mathbf{k}_l -point for the bands lower than the plane of Dirac nodal line. For the triplon bands in Fig.2(b)-(d) the topological invariant is $\Delta S_z = +2$. The non-zero topological invariant ensures the robustness of the Dirac nodal line in the presence of additional (perturbative)

interactions that do not break the $U(1)$ symmetry.

To verify that the nodal line is indeed protected by the $U(1)$ symmetry, we investigate the effects of several perturbations breaking different symmetries of the lattice. First, we include an in-plane magnetic field h_x along x-direction to illustrate the effect of $U(1)$ -symmetry breaking. This transforms the Hamiltonian Eq.4 as,

$$\mathcal{H} = \sum_{\mathbf{k}} \begin{pmatrix} \hat{t}_{\mathbf{k}}^{\bar{1}\dagger} \\ \hat{t}_{\mathbf{k}}^{\bar{0}\dagger} \\ \hat{t}_{\mathbf{k}}^{\bar{1}\dagger} \end{pmatrix} \begin{pmatrix} J - \gamma(\mathbf{k}) & -\frac{1}{\sqrt{2}}g_x h_x & 0 \\ -\frac{1}{\sqrt{2}}g_x h_x & J & -\frac{1}{\sqrt{2}}g_x h_x \\ 0 & -\frac{1}{\sqrt{2}}g_x h_x & J + \gamma(\mathbf{k}) \end{pmatrix} \begin{pmatrix} \hat{t}_{\mathbf{k}}^{\bar{1}} \\ \hat{t}_{\mathbf{k}}^{\bar{0}} \\ \hat{t}_{\mathbf{k}}^{\bar{1}} \end{pmatrix}, \quad (8)$$

where g_x is the g-factor and for simplicity we assume $g_x = g_z$. The eigenvalues of the Hamiltonian Eq.8 are $J \pm d(\mathbf{k})$, J , where $d(\mathbf{k}) = (\gamma(\mathbf{k})^2 + (g_z h_x)^2)^{1/2}$. The triplon bands in presence of in plane magnetic field h_x (Fig.3) shows that the degeneracies at the Dirac nodal line is lifted.

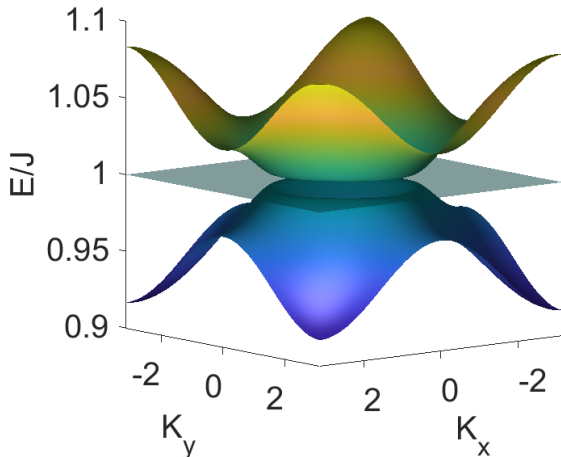


FIG. 3: **$U(1)$ symmetry breaking.** The triplon band structure for $h_z = h_c/2$, $h_x = h_c/10$. For better visibility the middle band is kept transparent.

Conservation of time-reversal symmetry along with the $U(1)$ -symmetry further restricts that the nodal line can not be gapped out. In presence of time-reversal symmetry breaking term which preserves the $U(1)$ symmetry, the equivalency between the states $|t^1\rangle$ and $|t^{\bar{1}}\rangle$ is lifted and so tuning such parameter, the nodal line degeneracy can be lifted. As we can see in figure Fig.2(a),(e) the nodal line degeneracy is lifted tuning the perpendicular magnetic field which preserves the $U(1)$ -symmetry but breaks the time reversal symmetry of the system.

The underlying Shastry-Sutherland lattice and the parent hamiltonian possess additional symmetries, including C_4 rotation about an axis perpendicular to the plane of the lattice and passing through the center of an empty plaquette and a $\mathcal{G} \otimes \mathcal{T}$ symmetry, consisting of glide plane and time reversal symmetry operations. The choice of perpendicular DM-interactions $D_{\perp,x}$ and $D_{\perp,y}$ as shown in Fig.4(a), with $D_{\perp,x} \neq D_{\perp,y}$ breaks the $\mathcal{G} \otimes \mathcal{T}$ and C_4 -symmetries. The dispersion of the triplon bands in the presence of such a symmetry breaking perturbation is given by $J - \nu\gamma'(\mathbf{k}) + J_3 \cos(k_x) \cos(k_y)$, where we have also added a third nearest neighbor Heisenberg exchange interaction J_3 (shown by black dotted line in Fig.4(a)) that does not break any symmetry of the system. Here $\nu = +1, -1, 0$ for $|t^1\rangle$, $|t^0\rangle$ and $|t^{\bar{1}}\rangle$ respectively and $\gamma'(\mathbf{k}) = g_z h_z + D_{\perp,x} \cos(k_x) + D_{\perp,y} \cos(k_y)$. The band structures for $D_{\perp,x} \neq D_{\perp,y}$ is shown in Fig.4(b), (c), where the nodal lines are still protected by $U(1)$ and \mathcal{T} symmetry. The Heisenberg-interaction J_3 changes the band dispersion of the three different triplon species exactly same way and so the nodal line is not lifted in presence of J_3 as shown in Fig.4(d).

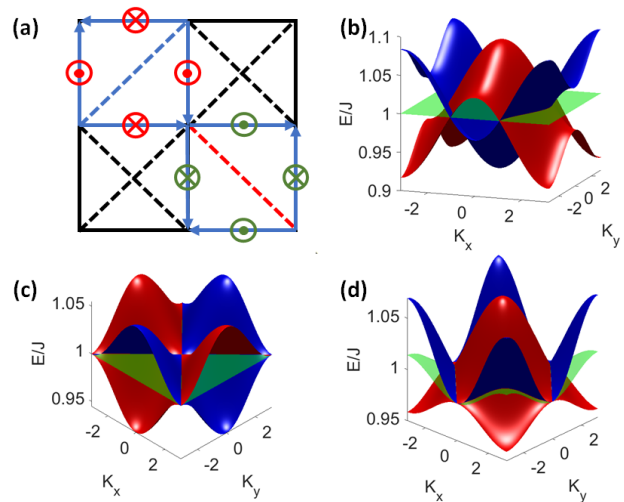


FIG. 4: **$U(1) \otimes \mathcal{T}$ symmetry protected nodal line.** (a) The red and blue circled dots or cross denotes the interaction $D_{\perp,x}$ and $D_{\perp,y}$. The black dotted lines denote the third Heisenberg interaction. The band structure for (b) $D_{\perp,y} = 2D_{\perp,x} = -40GHz$, $J_3 = 0GHz$; (c) $D_{\perp,y} = -D_{\perp,x} = -20GHz$, $J_3 = 0GHz$; (d) $D_{\perp,y} = D_{\perp,x} = -20GHz$, $J_3 = 10GHz$. For all the band structure the other parameters are $J = 722GHz$, $g_z = 2.28GHz$, $h_z = 0$

V. CONCLUSION

We have shown that triplon Dirac nodal line appears in the magnetic excitation spectrum of a microscopic model of $SrCu_2(BO_3)_2$ in its high symmetry phase using experimentally determined hamiltonian parameters. Whereas the previous studies showed the presence of nodal lines in the excitation spectrum of **classical spin states**, this study shows that the Dirac nodal lines also exist in the excitations of the short-range ordered purely quantum dimerized ground state of Shastry-Sutherland lattice. Our results demonstrate that the nodal lines are protected by a $U(1)$ and time reversal symmetries and is robust against any perturbation that do not break both of them. The nodal lines also persist in the presence of weak time reversal symmetry breaking fields. In an applied longitudinal magnetic field, the nodal lines continually shrink and eventually disappear at a critical field. In contrast to previous studies that explore prototypical models of certain classes of quantum magnets, our results are based on a faithful microscopic model of a (quasi 2D) real magnet. This novel Dirac nodal loop can be observed via inelastic neutron scattering experiment in the high crystal symmetry phase of $SrCu_2(BO_3)_2$, when all the in-plane DM-interactions are disallowed by symmetry of the crystal geometry thus protecting the $U(1)$ -symmetry of the spin-system. The presence of $U(1)$ -symmetry assures the presence of the Dirac nodal line and so it is expected that at higher temperature the triplon-triplon interac-

tions (which has not been considered in our study) can not remove the Dirac-nodal line[73–75].

Financial support from the Ministry of Education, Singapore, in the form of grant MOE2018-T1-001-021 is gratefully acknowledged.

-
- [1] B. Q. Lv, H. M. Weng, B. B. Fu, X. P. Wang, H. Miao, J. Ma, P. Richard, X. C. Huang, L. X. Zhao, G. F. Chen, Z. Fang, X. Dai, T. Qian, and H. Ding, *Phys. Rev. X* **5**, 031013 (2015).
- [2] H. Weng, C. Fang, Z. Fang, B. A. Bernevig, and X. Dai, *Phys. Rev. X* **5**, 011029 (2015).
- [3] S.-M. Huang, S.-Y. Xu, I. Belopolski, C.-C. Lee, G. Chang, B. Wang, N. Alidoust, G. Bian, M. Neupane, C. Zhang, S. Jia, A. Bansil, H. Lin, and M. Z. Hasan, *Nature Communications* **6**, 7373 (2015).
- [4] A. A. Burkov, M. D. Hook, and L. Balents, *Phys. Rev. B* **84**, 235126 (2011).
- [5] G. Xu, H. Weng, Z. Wang, X. Dai, and Z. Fang, *Phys. Rev. Lett.* **107**, 186806 (2011).
- [6] C. Fang, Y. Chen, H.-Y. Kee, and L. Fu, *Phys. Rev. B* **92**, 081201 (2015).
- [7] Y. Kim, B. J. Wieder, C. L. Kane, and A. M. Rappe, *Phys. Rev. Lett.* **115**, 036806 (2015).
- [8] R. Yu, H. Weng, Z. Fang, X. Dai, and X. Hu, *Phys. Rev. Lett.* **115**, 036807 (2015).
- [9] Y. Huh, E.-G. Moon, and Y. B. Kim, *Phys. Rev. B* **93**, 035138 (2016).
- [10] J.-W. Rhim and Y. B. Kim, *Phys. Rev. B* **92**, 045126 (2015).
- [11] Y. Wu, L.-L. Wang, E. Mun, D. D. Johnson, D. Mou, L. Huang, Y. Lee, S. L. Bud'ko, P. C. Canfield, and A. Kaminski, *Nature Physics* **12**, 667 (2016), [arXiv:1603.00934 \[cond-mat.mtrl-sci\]](https://arxiv.org/abs/1603.00934).
- [12] G. Bian, T.-R. Chang, R. Sankar, S.-Y. Xu, H. Zheng, T. Neupert, C.-K. Chiu, S.-M. Huang, G. Chang, I. Belopolski, D. Sanchez, M. Neupane, N. Alidoust, C. Liu, B. Wang, C.-C. Lee, H.-T. Jeng, C. Zhang, Z. Yuan, and M. Z. Hasan, *Nature Communications* **7**, 10556 (2016).
- [13] G. Bian, T.-R. Chang, H. Zheng, S. Velury, S.-Y. Xu, T. Neupert, C.-K. Chiu, S.-M. Huang, D. S. Sanchez, I. Belopolski, N. Alidoust, P.-J. Chen, G. Chang, A. Bansil, H.-T. Jeng, H. Lin, and M. Z. Hasan, *Phys. Rev. B* **93**, 121113 (2016).
- [14] L. M. Schoop, M. N. Ali, C. Straer, A. Topp, A. Varykhalov, D. Marchenko, V. Duppel, S. S. P. Parkin, B. V. Lotsch, and C. R. Ast, *Nature Communications* **7** (2016), 10.1038/ncomms11696.
- [15] M. Neupane, I. Belopolski, M. M. Hosen, D. S. Sanchez, R. Sankar, M. Szlawska, S.-Y. Xu, K. Dimitri, N. Dhakal, P. Maldonado, P. M. Oppeneer, D. Kaczorowski, F. Chou, M. Z. Hasan, and T. Durakiewicz, *Phys. Rev. B* **93**, 201104 (2016).
- [16] Q. D. Gibson, L. M. Schoop, L. Muechler, L. S. Xie, M. Hirschberger, N. P. Ong, R. Car, and R. J. Cava, *Phys. Rev. B* **91**, 205128 (2015).
- [17] S.-Y. Yang, H. Yang, E. Derunova, S. S. P. Parkin, B. Yan, and M. N. Ali, *Advances in Physics: X* **3**, 1414631 (2018), <https://doi.org/10.1080/23746149.2017.1414631>.
- [18] Y.-H. Chan, C.-K. Chiu, M. Y. Chou, and A. P. Schnyder, *Phys. Rev. B* **93**, 205132 (2016).
- [19] K.-H. Jin, H. Huang, Z. Wang, and F. Liu, *Nanoscale* **11**, 7256 (2019).
- [20] Y.-T. Oh, H.-G. Min, and Y. Kim, *Phys. Rev. B* **99**, 201110 (2019).
- [21] D. Shao, T. Chen, Q. Gu, Z. Guo, P. Lu, J. Sun, L. Sheng, and D. Xing, *Scientific Reports* **8** (2017), 10.1038/s41598-018-19870-5.
- [22] T. Ozawa, H. M. Price, A. Amo, N. Goldman, M. Hafezi, L. Lu, M. C. Rechtsman, D. Schuster, J. Simon, O. Zeitlinger, and I. Carusotto, *Rev. Mod. Phys.* **91**, 015006 (2019).
- [23] W. Gao, B. Yang, B. Tremain, H. Liu, Q. Guo, L. Xia, A. Hibbins, and S. Zhang, *Nature Communications* **9** (2018), 10.1038/s41467-018-03407-5.
- [24] S. Klembt, T. H. Harder, O. A. Egorov, K. Winkler, R. Ge, M. A. Bandres, M. Emmerling, L. Worschech, T. C. H. Liew, M. Segev, and et al., *Nature* **562**, 552556 (2018).
- [25] T. Karzig, C.-E. Bardyn, N. H. Lindner, and G. Refael, *Phys. Rev. X* **5**, 031001 (2015).
- [26] S. A. Owerre, *Journal of Physics: Condensed Matter* **28**, 386001 (2016).
- [27] D. Bhowmick and P. Sengupta, “The topological magnon bands in the flux state in sashtry-sutherland lattice,” (2020), [arXiv:2001.07008 \[cond-mat.str-el\]](https://arxiv.org/abs/2001.07008).
- [28] D. Malz, J. Knolle, and A. Nunnenkamp, *Nature Communications* **10** (2019), 10.1038/s41467-019-11914-2.
- [29] M. Malki and G. S. Uhrig, *Phys. Rev. B* **99**, 174412 (2019).
- [30] M. Kawano and C. Hotta, *Phys. Rev. B* **99**, 054422 (2019).
- [31] D. Joshi, *Physical Review B* **98** (2018), 10.1103/PhysRevB.98.060405.
- [32] D. Joshi and A. Schnyder, *Physical Review B* **100** (2019), 10.1103/PhysRevB.100.020407.
- [33] K. H. Lee, S. B. Chung, K. Park, and J.-G. Park, *Phys. Rev. B* **97**, 180401 (2018).
- [34] S. K. Kim, H. Ochoa, R. Zarzuela, and Y. Tserkovnyak, *Phys. Rev. Lett.* **117**, 227201 (2016).
- [35] D. Bhowmick and P. Sengupta, “Anti-chiral edge states in heisenberg ferromagnet on a honeycomb lattice,” (2019), [arXiv:1908.04580 \[cond-mat.str-el\]](https://arxiv.org/abs/1908.04580).
- [36] R. Chisnell, J. S. Helton, D. E. Freedman, D. K. Singh, R. I. Bewley, D. G. Nocera, and Y. S. Lee, *Phys. Rev. Lett.* **115**, 147201 (2015).
- [37] R. Seshadri and D. Sen, *Phys. Rev. B* **97**, 134411 (2018).
- [38] F.-Y. Li, Y.-D. Li, Y. B. Kim, L. Balents, Y. Yu, and G. Chen, *Nature Communications* **7** (2016), 10.1038/ncomms12691.
- [39] K.-K. Li and J.-P. Hu, *Chinese Physics Letters* **34**, 077501 (2017).
- [40] T. Liu and Z. Shi, *Physical Review B* **99** (2019), 10.1103/physrevb.99.214413.
- [41] S. A. Owerre, *Phys. Rev. B* **97**, 094412 (2018).
- [42] S.-K. Jian and W. Nie, *Phys. Rev. B* **97**, 115162 (2018).
- [43] S. Owerre, *Annals of Physics* **406**, 14 (2019).

- [44] P. Shen and S. K. Kim, *Phys. Rev. B* **101**, 125111 (2020).
- [45] S. Park and B.-J. Yang, *Phys. Rev. B* **99**, 174435 (2019).
- [46] S. Zhang, G. Go, K.-J. Lee, and S. K. Kim, “Su(3) topology of magnon-phonon hybridization in 2d antiferromagnets,” (2019), [arXiv:1909.08031](https://arxiv.org/abs/1909.08031) [cond-mat.mes-hall].
- [47] G. Go, S. K. Kim, and K.-J. Lee, *Phys. Rev. Lett.* **123**, 237207 (2019).
- [48] A. Mook, J. Henk, and I. Mertig, *Phys. Rev. B* **95**, 014418 (2017).
- [49] K. Li, C. Li, J. Hu, Y. Li, and C. Fang, *Phys. Rev. Lett.* **119**, 247202 (2017).
- [50] S. A. Owerre, *EPL (Europhysics Letters)* **125**, 36002 (2019).
- [51] L. Petersen and P. Hedegrd, *Surface Science* **459**, 49 (2000).
- [52] J.-L. Lu, W. Luo, X.-Y. Li, S.-Q. Yang, J.-X. Cao, X.-G. Gong, and H.-J. Xiang, *Chinese Physics Letters* **34**, 057302 (2017).
- [53] Y.-J. Jin, R. Wang, J.-Z. Zhao, Y.-P. Du, C.-D. Zheng, L.-Y. Gan, J.-F. Liu, H. Xu, and S. Y. Tong, *Nanoscale* **9**, 13112 (2017).
- [54] B. Feng, F. Botao, S. Kasamatsu, S. Ito, P. Cheng, C. Liu, Y. Feng, S. Wu, S. Mahatha, P. Sheverdyeva, P. Moras, M. Arita, O. Sugino, T.-C. Chiang, K. Shimada, K. Miyamoto, T. Okuda, K. Wu, L. Chen, and I. Matsuda, *Nature Communications* **8**, 1007 (2017).
- [55] S. A. Owerre, *Scientific Reports* **7** (2017), [10.1038/s41598-017-07276-8](https://doi.org/10.1038/s41598-017-07276-8).
- [56] B. S. Shastry and B. Sutherland, *Physica B+C* **108**, 1069 (1981).
- [57] R. W. Smith and D. A. Keszler, *Journal of Solid State Chemistry* **93**, 430 (1991).
- [58] K. Sparta, G. Redhammer, P. Roussel, G. Heger, G. Roth, P. Lemmens, A. Ionescu, M. Grove, G. Güntherodt, F. Hüning, *et al.*, *The European Physical Journal B-Condensed Matter and Complex Systems* **19**, 507 (2001).
- [59] J. Romhányi, K. Totsuka, and K. Penc, *Phys. Rev. B* **83**, 024413 (2011).
- [60] S. Miyahara and K. Ueda, *Phys. Rev. Lett.* **82**, 3701 (1999).
- [61] A. Koga and N. Kawakami, *Phys. Rev. Lett.* **84**, 4461 (2000).
- [62] A. Läuchli, S. Wessel, and M. Sigrist, *Phys. Rev. B* **66**, 014401 (2002).
- [63] J. Romhányi, K. Penc, and R. Ganesh, *Nature Communications* **6**, 6805 (2015), [arXiv:1406.1163](https://arxiv.org/abs/1406.1163) [cond-mat.str-el].
- [64] M. Malki and K. P. Schmidt, *Phys. Rev. B* **95**, 195137 (2017).
- [65] P. A. McClarty, F. Krüger, T. Guidi, S. F. Parker, K. Refson, A. W. Parker, D. Prabhakaran, and R. Coldea, *Nature Physics* **13**, 736 (2017), [arXiv:1609.01922](https://arxiv.org/abs/1609.01922) [cond-mat.str-el].
- [66] H. Kageyama, K. Yoshimura, R. Stern, N. V. Mushnikov, K. Onizuka, M. Kato, K. Kosuge, C. P. Slichter, T. Goto, and Y. Ueda, *Phys. Rev. Lett.* **82**, 3168 (1999).
- [67] C. Knetter, A. Bühler, E. Müller-Hartmann, and G. S. Uhrig, *Phys. Rev. Lett.* **85**, 3958 (2000).
- [68] S. Miyahara and K. Ueda, *Phys. Rev. B* **61**, 3417 (2000).
- [69] S. Sachdev and R. N. Bhatt, *Phys. Rev. B* **41**, 9323 (1990).
- [70] H. Nojiri, H. Kageyama, Y. Ueda, and M. Motokawa, *Journal of the Physical Society of Japan* **72**, 3243 (2003).
- [71] O. b. u. Türker and S. Moroz, *Phys. Rev. B* **97**, 075120 (2018).
- [72] C. Fang, H. Weng, X. Dai, and Z. Fang, *Chinese Physics B* **25**, 117106 (2016).
- [73] S. S. Pershoguba, S. Banerjee, J. C. Lashley, J. Park, H. Ågren, G. Aeppli, and A. V. Balatsky, *Phys. Rev. X* **8**, 011010 (2018).
- [74] *Nuclear Physics B* **424**, 595 (1994).
- [75] D. C. Elias, R. V. Gorbachev, A. S. Mayorov, S. V. Morozov, A. A. Zhukov, P. Blake, L. A. Ponomarenko, I. V. Grigorieva, K. S. Novoselov, F. Guinea, and et al., *Nature Physics* **7**, 701704 (2011).